Chemical Engineering Journal 162 (2010) 424–429

Contents lists available at ScienceDirect

Chemical Engineering Journal

journal homepage: www.elsevier.com/locate/cej

Short communication

Hybrid isotherms for adsorption and capillary condensation of N_2 at 77 K on porous and non-porous materials

K. Vasanth Kumar[a,*], C. Valenzuela-Calahorro[b], J.M. Juarez[a], M. Molina-Sabio[a], J. Silvestre-Albero[a], F. Rodriguez-Reinoso[a]

[a] Laboratorio de Materiales Avanzados, Departamento de Química Inorgánica, Uiversidad de Alicante, Apartado 99; E-03080 Alicante, Spain
[b] Departamento de Química Inorgánica, Facultad de Farmacia, Universidad de Granada, E-18071 Granada, Spain

ARTICLE INFO

Article history:
Received 3 February 2010
Received in revised form 29 April 2010
Accepted 30 April 2010

Keywords:
Adsorption
Capillary condensation
N_2
Equilibrium
Hybrid isotherms

ABSTRACT

A simple hybrid isotherm, which is an addition of Frenkel–Halsey–Hill isotherm to the Redlich–Peterson (RPFHH) isotherm, is proposed, taking into account the theoretical limitations of these models. The hybrid isotherm was fitted to N_2 adsorption isotherm (at 77 K) on porous and non-porous materials that involve only an adsorption step or an additional step due to condensation of the gas molecules on large pores. The RPFHH isotherm was found to be the successful in representing the N_2 adsorption isotherm of any type of porous and non-porous materials over the whole range of relative pressure range. The RPFHH isotherm can be adjusted to identify the adsorption process besides the condensation process, allowing to determine the theoretical sorption capacity. The surface area of the materials predicted by the RPFHH was in general in good agreement with the values obtained by the BET method.

1. Introduction

Porous materials are characterized mainly by the presence of three types of pores, micropores (<2 nm), mesopores (2–50 nm) and macropores (>50 nm) according to the recommendation of the IUPAC [1]. The use of nitrogen adsorption isotherms at 77 K is the starting point for the characterization of adsorbents [1]. A BET plot in the relative pressure p/p_o range of 0.03–0.30 is commonly used for the analysis of surface area and several approaches can be used to determine the different pore volumes [1]. Few empirical isotherms have been developed for condensable vapors and they are reviewed elsewhere [1,2]. However, the range of relative pressure for the applicability of these models could vary depending on the adsorbent properties. Many of existing models are successful in representing: (i) the adsorption isotherm at low pressures prior to monolayer coverage; (ii) monolayer coverage in the region of relatively higher pressure; and (iii) multilayer and capillary condensation of condensable vapors in the region of higher relative pressures [1–6]]. For practical application, it would be more useful to understand the adsorption equilibria over a broad range of pressure and temperature. Thus any isotherm representing adsorption equilibrium for a wide range of relative pressures could provide information in the dynamic simulation needed for the design of adsorption facilities [5].

Recently, Shim et al. [4] made an attempt to model the adsorption of volatile organic compounds (VOC) onto mesoporous silicas, MCM-48 and MCM-41 at different temperatures (303.15–323.15 K) using a hybrid isotherm consisting of Langmuir and Sips isotherms. Casas et al. [7] modeled the equilibrium adsorption data of xanthine derivatives on activated carbon at different temperatures (283–323 K), assuming multiple adsorption steps and one condensation process. However, the mathematical uncertainties and the theoretical limitations of these models were left unconsidered.

In this study, an attempt is made to present a hybrid isotherm that could represent the equilibrium data of N_2 onto different porous and non-porous materials at 77 K over a wide range of relative pressure. The hybrid isotherm presented in this study is constructed by combining the Redlich–Peterson isotherm at low relative pressure up to the monolayer coverage and the Frenkel–Halsey–Hill isotherm at higher pressure, corresponding to capillary condensation. Redlich–Peterson and Frenkel–Halsey–Hill isotherms are selected considering the theoretical strength of these models. Redlich-Peterson expression was selected because it is analogous to Henry and Langmuir isotherms at relatively low and high pressure, respectively. For a higher value of Redlich–Peterson isotherm constants, *A* and *B*, this isotherm could represent a Freundlich isotherm. Frenkel–Halsey–Hill isotherm was selected to represent the molecular layer condensation in the capillaries at higher relative pressures. A combination of Redlich–Peterson and Frenkel–Halsey–Hill isotherm would be a more reliable expression in representing the experimental isotherms of any type due to flexibility and the number of parameters involved in the isotherm

* Corresponding author.
E-mail addresses: vasanth@ua.es, vasanth_vit@yahoo.com (K.V. Kumar).

1385-8947/$ – see front matter © 2010 Elsevier B.V. All rights reserved.
doi:10.1016/j.cej.2010.04.058

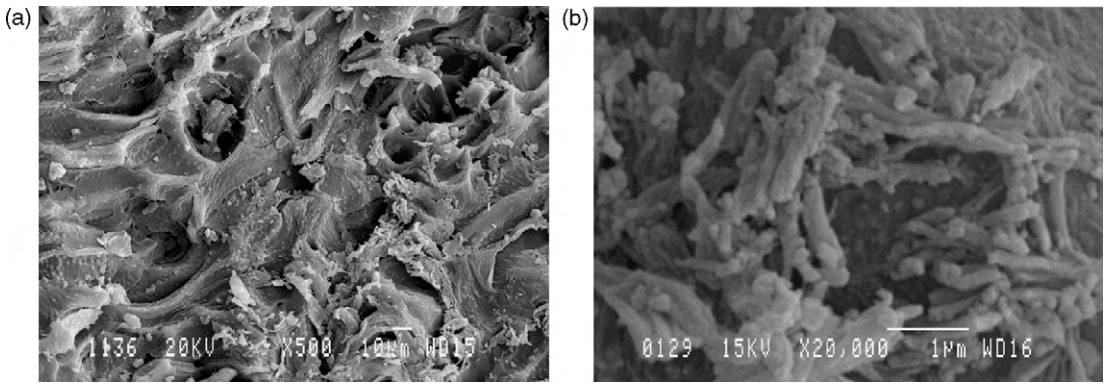

Fig. 1. SEM pictures of (a) D53 and (b) MCM-41.

expression. The equilibrium data of N_2 at 77 K on some porous and non-porous materials were selected as model systems as the experimental isotherms show the evidence of monolayer adsorption or both monolayer adsorption and capillary condensation at this temperature.

2. Experimental

Several adsorbents with different textural properties have been selected: (i) a non-porous graphitized carbon black, V3G, with a particle size of around 20 nm [8]; (ii) a granular essentially mesoporous carbon, LMA-15, prepared in our facilities by thermal activation of olive stones impregnated with a metal salt [9]; (iii) a mesoporous silica of the type of MCM-41 [10], with regular mesoporous cylindrical channels of around 3 nm prepared in our facilities following the traditional recipe of Matsumoto et al. [11]; and (iv) a series of essentially microporous activated carbons prepared in the laboratory by thermal activation (under a flow of carbon dioxide) of an olive stone char to different degrees of burn-off (8–80%) [8,12,13]. The porosity of this later series of activated carbons, obtained by adsorption of gases and hydrocarbons and by immersion calorimetry, are described elsewhere [8,12,13]. The SEM pictures for D52 and MCM-41 (Fig. 1a and b), as typical examples, show the different morphological characteristics of these adsorbents.

3. Theory

The three parameter Redlich–Peterson [14] isotherm includes the best features of Freundlich and Langmuir isotherms and it is given by

$$n = \frac{Ap}{1 + Bp^g} \tag{1}$$

where, A, B and g are the empirical coefficients of the Redlich–Peterson isotherm. The value of the exponent, g lies in the range 0–1. The Redlich-Peterson isotherm converges to Langmuir, Henry and Freundlich isotherm for the conditions: (i) $g = 1$, (ii) $g = 0$ and (iii) A and $B \gg 1$ and $g < 1$, respectively [14–16].

Frenkel [17], Halsey [18] and Hill [19] independently suggested that at high relative pressures, where the adsorbed film is several molecular layers in thickness and its properties approach those of the bulk liquid, the isotherm could be represented by the expression

$$-\ln\left(\frac{p}{p_o}\right) = \frac{k}{\left(V/V_m\right)^s} \tag{2}$$

Rearranging Eq. (2) and dividing both sides by the density of adsorbed phase, it can be written in terms of moles adsorbed

$$n = n_m\left(-\frac{k}{\ln(p/p_o)}\right)^{1/s} \tag{5}$$

where, k, p_o and V_m refer to a positive constant, the saturation vapor pressure and micropore volume, respectively. The exponent s is based on the decay of surface forces with distance.

In this study, the isotherms of several porous materials are characterized by a hybrid isotherm, which is addition of a Frenkel–Halsey–Hill isotherm to the Redlich–Peterson isotherm

$$n = n_m\left(\frac{Ap}{1 + Bp^g} + \left(-\frac{k}{\ln(p/p_o)}\right)^{1/s}\right) \tag{6}$$

The hybrid isotherm was obtained on the assumption of the sorption process involving multiple steps that could explain monolayer and multilayer sorption including the capillary condensation process. Eq. (6) is theoretically flexible and could represent the Henry, Freundlich, Langmuir isotherms and the multilayer sorption involving the capillary condensation process.

In addition to the hybrid isotherm presented in Eq. (6), the classical Frenkel–Halsey–Hill isotherm and several hybrid isotherms presented by other researchers for different adsorption systems are tried and the results are given in Table 1.

4. Results and discussion

Fig. 2 shows the experimental data and the predicted hybrid isotherms for nitrogen on non-porous graphitized carbon black, V3G by non-linear regression analysis method. The non-linear regression involves an error minimization procedure which was performed by maximizing the coefficient of determination, r^2, using the *solver* add-in function, Microsoft Spread sheet, Microsoft Excel between the experimental data and theoretical isotherms:

$$r^2 = \frac{\Sigma(n_{\text{isotherm}} - \overline{n_{\text{experimental}}})^2}{\Sigma(n_{\text{isotherm}} - \overline{n_{\text{experimental}}})^2 + \Sigma(n - n_{\text{isotherm}})^2} \tag{7}$$

The calculated isotherm parameters for nitrogen at 77 K on V3G and the optimized r^2 values are given in Table 2. It is shown that, although five hybrid isotherms are applied, the hybrid RPFHH was found is the best fit isotherm in representing type II isotherm (typical for non-porous solids), with higher r^2 values. In addition, the FHH isotherm itself correctly represents the experimental equilibrium data over the whole range of relative pressures studied. Irrespective of the larger number of parameters involved in L + F, S + F, RP + S, L + S, the lower r^2 values for these isotherms poorly represent the experimental equilibrium data over the range of relative pressures covered.

Table 1
Hybrid isotherms for N_2 adsorption onto porous and non-porous materials.

Isotherm	Equation	Mathematical limitations	Source
Frenkel–Halsey–Hill	$n = n_m\left(-\frac{k_{FHH}}{\ln(p/p_o)}\right)^{1/s}$	k_{FHH}: a positive constant	[1,17–19]
Sips + Freundlich	$n = n_m\left(\frac{Bp^g}{1+Bp^g} + k_f p^{n_f}\right)$	$0 < g < 1$	[6,20–21]
Redlich–Peterson + Frenkel–Halsey–Hill	$n = n_m\left(\frac{Bp}{1+Bp^g} + \left(-\frac{k_{FHH}}{\ln(p/p_o)}\right)^{1/s}\right)$	$0 < g < 1$	This study
Langmuir + Freundlich	$n = n_m\left(\frac{k_L p}{1+k_L p} + k_f p^{n_f}\right)$		This study
Redlich–Peterson + Sips	$n = n_m\left(\frac{Bp}{1+Bp^g} + \frac{k_s p^{m_s}}{1+k_s p^{m_s}}\right)$	$-1 < m_s + 1; 0 < g < 1$	This study
Langmuir + Sips	$n = n_m\left(\frac{k_L p}{1+k_L p} + \frac{k_s p^{m_s}}{1+k_s p^{m_s}}\right)$	$-1 < m_s < +1$	[3,20–22]

In the case of adsorption of nitrogen on carbon LMA-15, a large amount was adsorbed at relatively higher pressure (Type IV isotherm), which is typically due to the presence of mesoporosity (Fig. 3). The adsorption and desorption path are not coincident, exhibiting a hysterisis loop above $p/p_o = 0.4$. Fig. 3 also shows the fitted isotherms onto the experimental data by a non-linear regression technique and it can be observed that RPFHH and FHH isotherms are the best fitting isotherms in representing a type IV isotherm for LMA-15. For this adsorbent, the r^2 of FHH isotherm was found to be relatively higher than the r^2 of RPFHH isotherm.

Table 2
Isotherm parameters determined by non-linear regression analysis for N_2 onto porous and non-porous materials studied at 77 K.

Isotherm	Parameters	V3G	LMA15	MCM41	D8	D19	D34	D52	D70	D80
	BET surface area	62	1021	886	647	797	989	1271	1426	1525
FHH	n_m	1.05E−03	1.04E−02	1.29E−02	7.16E−03	8.85E−03	1.13E−02	1.47E−02	1.85E−02	1.94E−02
	k_{FHH}	0.995	2.632	1.074	1.256	1.281	1.396	1.274	1.333	1.272
	$1/s$	0.404	0.394	0.206	0.034	0.050	0.123	0.080	0.236	0.126
	Surface area	103	1014	1263	699	863	1104	1432	1805	1894
	r^2	0.997	0.972	0.647	0.869	0.872	1103.535	0.776	0.884	0.735
	95% CI	1.02E−04	2.16E−03	5.44E−03	1.02E−03	1.22E−03	6.05E−04	4.41E−03	6.58E−04	8E−03
S + F	n_m	1.96E−06	4.12E−06	1.70E−02	5.14E−03	2.20E−03	6.75E−03	3.60E−03	4.19E−03	9.40E−04
	k_s	2.11E−01	3.89E−02	9.91E−03	2.46E+00	1.78E+00	3.39E+00	1.05E+00	2.72E−02	2.96E−02
	n_s	0.950192	0.93913	1	1.00E+00	1	1	1	1	1
	k_F	0.088	0.052	0.278	0.250	2.373	0.358	2.123	2.684	12.077
	n_F	1.594928	1.87686	0	1.01E−01	0.053617	0.124675	0.083547	0.05986	0.111292
	r^2	0.689	0.966	0.977	0.998	0.996	0.999	0.997	0.999	0.994
	95% CI	7.66E−03	7.69E−03	8.35E−07	1.07E−05	5.49E−03	3.06E−5	6.11E−05	1.07E−05	9.81E−05
RP + FHH	n^m	6.45E−04	1.05E−02	9.08E−03	6.33E−03	4.72E−03	4.50E−03	8.25E−03	1.04E−02	1.25E−02
	B	3.30E−04	7.86E−04	2.90E−02	3.58E+00	4.14E+00	3.29E+00	1.10E−01	3.72E−02	2.32E−02
	A	2.13E−07	8.22E−06	2.63E−04	2.27E−02	1.96E−02	1.48E−02	9.08E−04	3.86E−04	2.91E−04
	g	1	1	0.913807	9.73E−01	0.9504	0.918052	1	1	1
	k_{FHH}	2.92E+00	1.56E+00	9.16E−07	9.99E−07	1.46E−06	2.01E+00	4.74E−01	1.93E+00	8.53E−03
	$1/s$	4.10E−01	4.16E−01	4.92E−02	4.12E−01	3.45E−02	0.00E+00	1.71E−02	0.00E+00	1.14E−02
	Surface area	63	1021	886	618	460	439	805	1014	1221
	r^2	0.998	0.970	0.966	0.999	0.998	0.999	0.945	0.977	0.991
	95% CI	2.82E−05	4.83E−03	1.32E−04	9.41E−06	5.31E−05	4.77E−05	8.16E−04	3.68E−04	6.05E−4
L + F	n_m	8.94E−07	2.20E−03	1.69E−02	1.61E−03	1.56E−03	6.22E−03	1.95E−03	2.83E−03	3.09E−03
	k_L	2.40E−02	51.196	0.010	4.12E−02	3.728	3.354	0.061	1.310	47.292
	k_F	0.050	0.000	0.277	3.695	3.592	0.464	5.262	3.083	2.690
	n_F	1.802	2.432	0.003	0.000	0.056	0.111	0.056	0.115	0.150
	r^2	0.704	0.904	0.977	0.987	0.999	0.999	0.999	0.992	0.994
	95% CI	6.76E−03	7.39E−03	2.20E−06	7.63E−05	8.69E−06	8.36E−06	5.27E−06	3.71E−05	4.19E−05
RP + S	n_m	7.57E−01	5.70E−02	2.02E−02	7.05E−03	6.99E−03	1.00E−02	9.34E−03	1.11E−02	1.28E−02
	B	1.2E−05	0.000692	0.022193	1.639799	6.062217	2.312519	10.59678	21.85782	6.449332
	A	9.11E−06	3.94E−05	0.000447	0.011564	0.042348	0.023139	0.098996	0.241718	0.082756
	g	1	1	1	0.999868	0.999994	0.999846	0.999125	1	1
	k_s	4.33E−08	8.17E−08	0.000699	0.000143	0.092213	0.008579	0.179206	0.07027	0.027012
	m_s	1.000	2.432	0.499	1.000	0.296	0.554	0.454	0.679	0.837
	r^2	0.635	0.772	0.940	0.999	1.000	0.999	1.000	1.000	1.000
	95% CI	1.56E−02	2.76E−02	1.88E−03	4.78E−06	2.89E−06	2.51E−05	3.50E−06	7.32E−05	2.47E−06
L + S	$n_m = A/B$	7.59E−01	5.69E−02	2.01E−02	7.05E−03	6.99E−03	1.00E−02	9.34E−03	1.11E−02	1.28E−02
	k_L	1.2E−05	0.000692	0.022193	1.639799	6.062217	2.312519	10.59678	21.85782	6.449332
	k_s	4.33E−08	8.17E−08	0.000699	0.000143	0.092213	0.008579	0.179206	0.07027	0.027012
	m_s	1.000	2.432	0.499	1.000	0.296	0.554	0.454	0.679	0.837
	r^2	0.635	0.772	0.940	0.999	1.000	0.999	1.000	1.000	1.000
	95% CI	1.54E−02	2.74E−02	1.85E−03	4.15E−06	2.51E−06	2.08E−05	3.13E−06	6.68E−06	2.26E−06
RP	A	5.58E−06	6.61E−5	5.14E−04	2.50E−02	1.83E−01	6.92E−02	6.41E−02	1.24E−01	1.28E−01
	B	1E−04	0	2.55E−02	3.971	25.694	7.831	5.821	10.931	10.971
	g	1	0.994	1	0.970	0.953	0.951	0.935	0.903	0.886
	R^2	0.747	0.766	0.937	0.998	0.998	0.999	0.997	0.992	0.992
	95% CI	1.01E−03	4.45E−02	1.01E−04	1.49E−05	9.25E−06	5.16E−06	1.99E−05	3.11E−05	1.10E−04

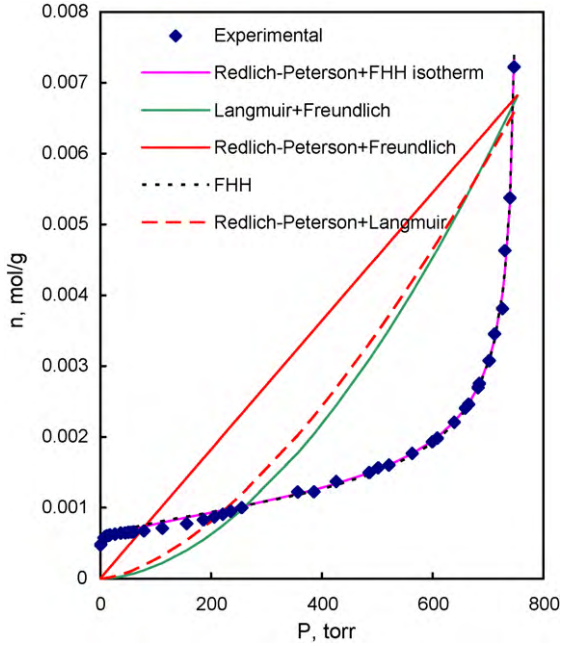

Fig. 2. Experimental data and predicted hybrid isotherms for N_2 onto V3G at 77 K.

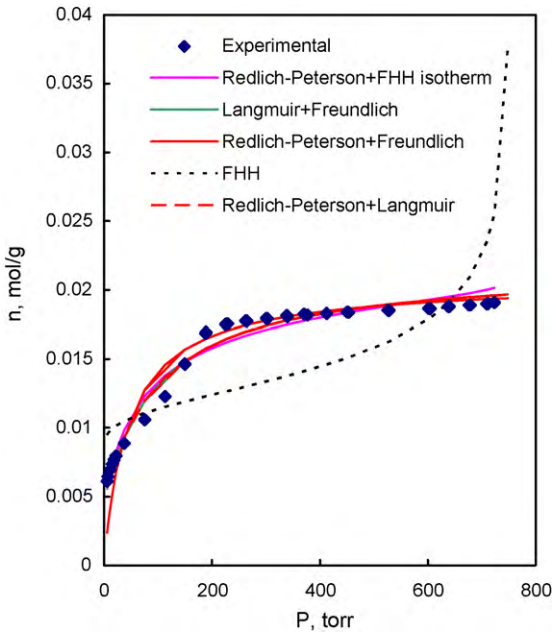

Fig. 4. Experimental data and predicted hybrid isotherms for N_2 onto MCM41 at 77 K.

This could be due to the influence of Redlich–Peterson isotherm parameter g, that was subjected to the constraint $0 < g < 1$ during the iteration procedure. The Redlich–Peterson isotherm can only represent the linear or exponential gas uptake and saturation at low and high pressures, respectively, (depending on the g value) and this model cannot explain the capillary condensation process. The parameter g subjected to constraints will adjust the experimental equilibrium data exhibiting the capillary condensation effect at higher pressures to represent the saturation during the iteration procedure, thus affecting the performance of the RPFHH expression. This could be realized from the lower r^2 value of RP isotherm for this adsorbent. The principle objective of this study is to find the suitable hybrid isotherm that could represent the equilibrium adsorption or capillary condensation process univocally and also to represent the equilibrium data involving both of these processes. The surface area calculated for carbon LMA-15 by both RPFHH and FHH isotherms over a wide range of relative pressures was in good agreement with the surface area determined by BET surface area method. The other hybrid isotherms used failed to represent the experimental equilibrium data and also to identify the multiple steps corresponding to monolayer adsorption and capillary condensation process for $p/p_o < 0.5$ and $p/p_o > 0.5$, respectively (Fig. 3).

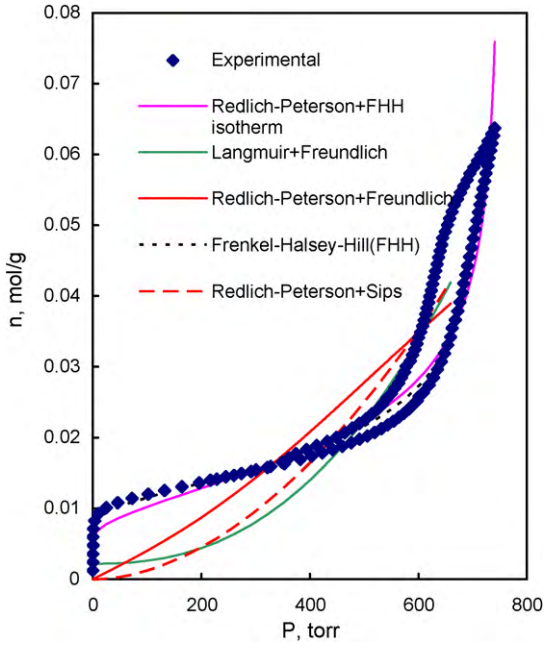

Fig. 3. Experimental data and predicted hybrid isotherms for N_2 onto LMA15 at 77 K.

The applicability of the proposed hybrid isotherm (RPFHH) for porous materials other than porous carbons was studied using the equilibrium data of N_2 at 77 K on a mesoporous silica (Fig. 4). The inflection at p/p_o roughly equal to 0.1 and a plateau at $p/p_o > 0.3$ indicate that adsorption occurs in mesopores of uniform size [1]. Fig. 4 shows that the FHH and RPFHH are the best fitting isotherms for the adsorption of N_2 onto MCM-41, with a higher r^2 value. The calculated isotherm parameters, surface area and the corresponding r^2 values are given in Table 2, where it is shown that the surface area of MCM-41 calculated using the maximum sorption capacity ($886\ m^2/g$) obtained from RPFHH isotherm was exactly the same as determined by the BET method. Table 2 also shows that the FHH isotherm over-estimates the surface area of MCM-41 at the conditions used.

The applicability of the proposed hybrid isotherm for type I isotherms which are typical of adsorbents with a predominantly microporous structure, was tested by fitting it to the N_2 adsorption isotherm (at 77 K) for a series of microporous carbons. Fig. 5 shows the experimental data and predicted isotherms for N_2 at 77 K on D-80 activated carbon. The FHH isotherm poorly represents the experimental data of N_2 on this microporous carbon, suggesting the inapplicability of this model for this adsorbent. The calculated isotherm parameters and the corresponding r^2 values are give in Table 2, where it is observed that all the hybrid isotherms studied fit the experimental equilibrium data of N_2 with higher r^2 value (Table 1). A similar effect was observed for the adsorption of N_2 on the rest of activated carbons of series—D (D-8, D-19, D-34, D-52 and D-70; the number gives the degree of activation of the carbon). In the case of RPFHH isotherm, the $1/s$ is lower than unity for the adsorption of N_2 on the adsorbents studied and to near zero for

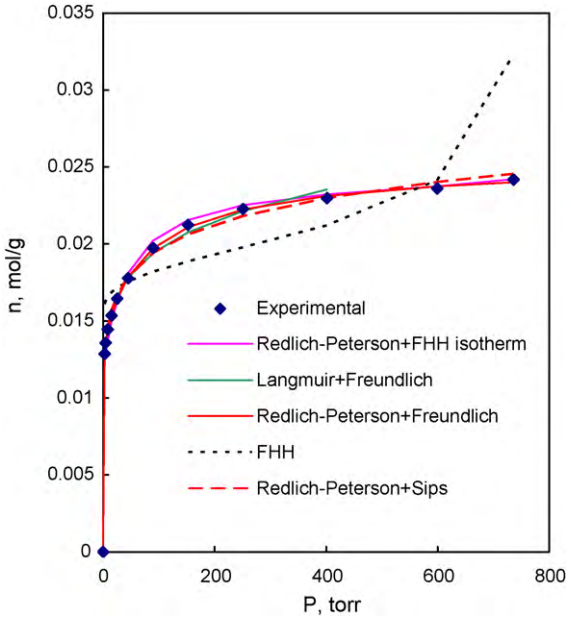

Fig. 5. Experimental data and predicted hybrid isotherms for N_2 onto D-80 activated carbon at 77 K.

D-34 and D-70, indicating that the experimental data are mainly represented by RP isotherm, with negligible contribution of the FHH isotherm. This shows the advantages of this model since the parameters of this model can be easily adjusted to represent the isotherm corresponding to adsorption or capillary condensation easily. In the case of microporous carbons (D-series), the theoretical adsorption capacity was found to be greatly influenced by the theoretical isotherms used. Considering the values of coefficient of determination, both RPS and RPFHH are found to be the best fit isotherms for N_2 on the series of microporous activated carbons studied, with r^2 value equal to unity.

The present study shows that a hybrid isotherm containing a Redlich–Peterson and Frenkel–Halsey–Hill isotherm could successfully represent type I, type II and type IV isotherms that are typical for microporous, non-porous and mesoporous materials, respectively, over a wide range of relative pressures. It is important to find an isotherm that is valid over a wide range of pressure because such expression can be used to simulate the dynamic behavior for the design of adsorption processes. The present study was aimed only to find a useful isotherm expression that could serve the purpose of explaining the adsorption isotherm over a wide range of relative pressures. It should be remembered that it may be a difficult process to get a physical insight of the process using hybrid isotherm, since the attempt made at this stage to combine two theoretical isotherms is at an empirical level. However this does not appear to be a serious drawback since the model parameters can be easily adjusted using a regression procedure and the resulting parameters can be used to explain the physical mechanism of adsorption process. The value of $1/s$ and g in the RPFHH isotherm can be used to identify the capillary condensation and the mechanism of the adsorption process simultaneously. The surface area of non-porous and mesoporous materials determined by RPFHH isotherm was found to be in good agreement with the surface area obtained by BET method. However, this model cannot be treated as universal expression for determining the surface area since it failed to predict the same for some of microporous adsorbents used in this study. The present study focuses only in identifying the adsorption and the condensation process using hybrid isotherms. Though in the present study, the applicability of the RPFHH isotherm is explained using the experimental isotherms of N_2 at 77 K, this isotherm can be applied to other adsorption systems exhibiting both adsorption and capillary condensation processes. Furthermore in this study no discussion was included with the micropore filling process and the process is assumed to involve either single step due to adsorption or multiple steps due to both adsorption and capillary condensation. The adsorption step was discussed based on the assumptions of RP isotherm that explain a heterogeneous or homogeneous adsorption process based on the g values and the condensation process was explained based on the limitations of FHH isotherm. No attempts have been made to correlate the determined isotherm parameters with the pore volumes of these established materials due to the physical or mathematical restrictions of the isotherm models adopted. The future study will be aimed to focus on these concepts by applying these hybrid isotherms to identify the multiple stages of adsorption in narrow and wide micropores simultaneously, considering the kinetic restrictions to the adsorptive molecules. At this stage the isotherm RPFHH can be used to globally represent any equilibrium data following type I, type II and type IV isotherms.

Acknowledgements

Support from the MEC (Projects MAT2004-03480-C02-02 and NAN2004-09267-C03-03) is gratefully acknowledged. Support from Generalitat Valenciana (project GRUPOS 03/212) is acknowledged. The work was carried out under the auspice of the European Network of Excellence InsidePores. KVK would like to thank Ministerio de Ciencia e Innovacion for the Juan de la Cierva contract. The valuable suggestions of the reviewers are appreciated and acknowledged.

References

[1] J. Rouquerol, F. Rouquerol, K.S.W. Sing, Adsorption by Powders and Porous Solids: Principles, Methodology and Applications, Academic Press, San Diego, CA, 1999.
[2] H. Marsh, F. Rodriguez-Reinoso, Activated Carbon, Elsevier Ltd., London, UK, 2006.
[3] J.W. Lee, W.G. Shim, H. Moon, Adsorption equilibrium and kinetics for capillary condensation of trichloroethylene on MCM-41 and MCM-48, Microporous and Mesoporous Materials 73 (3) (2004) 109–119.
[4] W.G. Shim, J.W. Lee, H. Moon, Adsorption equilibrium and column dynamics of VOCs on MCM-48 depending on pelletizing pressure, Microporous and Mesoporous Materials 88 (2006) 112–125.
[5] R.T. Yang, Adsorbents: Fundamentals and Applications, John Wiley & Sons, New York, 2003.
[6] A. Chakraborty, B.B. Saha, K.C. Ng, S. Koyama, K. Srinivasan, Theoretical insight of physical adsorption for a single-component adsorbent + adsorbate system: I. Thermodynamic property surfaces, Langmuir 25 (2009) 2204–2211.
[7] R.N. Casas, A.G. Rodriguez, F.R. Bueno, A.E. Lara, C.V. Calahorro, A.N. Guijosa, Interactions of xanthines with activated carbon: II. The adsorption equilibrium, Applied Surface Science 252 (2006) 6026–6030.
[8] M.T. Gonzalez, A. Sepulveda-Escribano, M. Molina-Sabio, F. Rodriguez-Reinoso, Correlation between surface areas and micropore volumes of activated carbons obtained from physical adsorption and immersion calorimetry, Langmuir 11 (1995) 2151–2155.
[9] J.C. Gonzalez, M.T. Gonzalez, M. Molina-Sabio, F. Rodriguez-Reinoso, A. Sepulveda-Escribano, Porosity of activated carbons preapared from different lignocellulosic materials, Carbon 33 (1995) 1175–1177.
[10] J. Silvestre-Albero, A. Sepulveda-Escribano, F. Rodriguez-Reinoso, Preaparation and characterization of Zn containing MCM-41 spheres, Microporous and Mesoporous Materials 113 (2008) 362–369.
[11] A. Matsumoto, H. Chen, K. Tsutsumi, M. Grun, K. Unger, Novel route in the synthesis of MCM-41 containing framework aluminum and its characterization, Microporous and Mesoporous Materials 32 (1999) 55–62.
[12] J. Garrido, A. Linares-Solano, J.M. Martin-Martinez, M. Molina-Sabio, F. Rodriguez-Reinoso, R. Torregrosa, Use of nitrogen vs. carbon dioxide in the characterization of activated carbons, Langmuir 3 (1987) 76–81.
[13] F. Rodriguez-Reinoso, J. Garrido, J.M. Martin-Martinez, M. Molina-Sabio, R. Torregrosa, The combined use of different approaches in the characterization of microporous carbons, Carbon 27 (1989) 23.
[14] O. Redlich, D.L. Peterson, A useful adsorption isotherm, Journal of Physical Chemistry 63 (1959) p1024.
[15] K.V. Kumar, Selection of optimum isotherm and kinetics of solid/liquid adsorption systems, PhD thesis, Anna University, 2007.
[16] K.V. Kumar, M. Monteiro de Castro, M. Martinez-Escandell, M. Molina-Sabio, J. Silvestre-Albero, F. Rodriguez-Reinoso, A continuous site energy distribu-

tion function from Redlich–Peterson isotherm for adsorption on heterogeneous surfaces, Chemical Physics Letters, in press, doi:10.1016/j.cplett.2010.04.044.
[17] J. Frenkel, Kinetic Theory of Liquids, Oxford University Press, 1946.
[18] G. Halsey, Physical adsorption on non-uniform surfaces, Journal of Chemical Physics 16 (10) (1948) 931–937.
[19] T.L. Hill, Thermodynamics of adsorption, Transactions of the Faraday Society 47 (1951) 376–380.
[20] R. Sips, On the structure of a catalyst surface. I, Journal of Chemical Physics 16 (5) (1948) 490–495.
[21] R. Sips, On the structure of a catalyst surface. II, Journal of Chemical Physics 18 (8) (1950) 1024–1026.
[22] I. Langmuir, The constitutions and fundamental properties of solids and liquids, Journal of the American Chemical Society 38 (11) (1916) 2221–2295.